Drosophila *domino* Exhibits Genetic Interactions with a Wide Spectrum of Chromatin Protein-Encoding Loci

Kaitlyn Ellis, Chloe Friedman, Barry Yedvobnick*

Biology Department, Emory University, Atlanta, Georgia, United States of America

* Barry.Yedvobnick@Emory.Edu

Abstract

The Drosophila *domino* gene encodes protein of the SWI2/SNF2 family that has widespread roles in transcription, replication, recombination and DNA repair. Here, the potential relationship of Domino protein to other chromatin-associated proteins has been investigated through a genetic interaction analysis. We scored for genetic modification of a *domino* wing margin phenotype through coexpression of RNAi directed against a set of previously characterized and more newly characterized chromatin-encoding loci. A set of other SWI2/SNF2 loci were also assayed for interaction with *domino*. Our results show that the majority of tested loci exhibit synergistic enhancement or suppression of the *domino* wing phenotype. Therefore, depression in *domino* function sensitizes the wing margin to alterations in the activity of numerous chromatin components. In several cases the genetic interactions are associated with changes in the level of cell death measured across the dorsal-ventral margin of the wing imaginal disc. These results highlight the broad realms of action of many chromatin proteins and suggest significant overlap with Domino function in fundamental cell processes, including cell proliferation, cell death and cell signaling.

Introduction

The Drosophila *domino* (*dom*) locus was initially characterized as a gene required for cell proliferation and viability, hematopoiesis and homeotic gene silencing [1,2]. The *dom* sequence predicts proteins of the SWI2/SNF2 class of DNA-dependent ATPases, implicating *dom* in gene regulation at the level of chromatin modification/nucleosome remodeling [2]. Domino proteins are widely expressed in embryos and imaginal tissues, and the sequence is highly conserved [2,3,4]. The locus has been associated with several functions, including exchange of phosphorylated histone H2Av as part of the Tip60 complex [3]. Tip60 is a lysine acetyltransferase, which acetylates histone and nonhistone proteins [5], and contributes to positive and negative gene regulation [6,7]. Dom function is also required in germline and somatic stem cells [8,9], and for repression of E2F responsive loci [10], Elongator complex target regulation [11] and Notch signaling [12,4,13,14]. Additionally, we previously described an RNAi-based, targeted screen for genetic modifiers of a *dom* wing phenotype [14]. This screen revealed several

major classes of interaction, including genes regulating RNA function, transcription, cell growth, proliferation and autophagy. The wide array of functions associated with *dom* indicate that the locus may be involved with diverse chromatin factors, however the identification of these factors is incomplete. Here we have initiated a genetic scheme to identify additional chromatin associated proteins that have a role within the larger functional network that includes Dom. We analyzed a set of previously-described and also more newly-characterized loci that encode chromatin-associated proteins [15,16], for genetic interaction with *dom* at the wing margin. We likewise analyzed other members of the *SWI2/SNF2* gene family [17]. Our results indicate that loss-of-function (LOF) for many of these proteins elicits synergistic biological effects with *dom*, demonstrating that depression of *dom* function sensitizes the wing margin to changes in the activity of a substantial fraction of these chromatin components.

Materials and Methods

Drosophila strains

The *C96-domR* and *C96-Gal4* strains were described previously [18,14]. The remaining strains listed below were obtained from the Bloomington (BL) Stock Center. The BL strain numbers are indicated within parentheses: *y[1] sc[*] v[1]; P{y[+t7.7] v[+t1.8] = TRiP.HMS00941}attP2* (33981), *y[1] sc[*] v[1]; P{y[+t7.7] v[+t1.8] = TRiP.HMS00919}attP2* (33962), *y[1] v[1]; P{y [+t7.7] v[+t1.8] = TRiP.JF02132}attP2* (26234), *y[1] v[1]; P{y[+t7.7] v[+t1.8] = TRiP.JF02211} attP2* (31921), *y[1] v[1]; P{y[+t7.7] v[+t1.8] = TRiP.HMJ02079}attP40* (42514), *y[1] v[1]; P{y [+t7.7] v[+t1.8] = TRiP.JF02212}attP2* (31922), *y[1] sc[*] v[1]; P{y[+t7.7] v[+t1.8] = TRiP. HMS00271}attP2* (33394), *y[1] sc[*] v[1]; P{y[+t7.7] v[+t1.8] = TRiP.HMS00676}attP2* (32888), *y[1] sc[*] v[1]; P{y[+t7.7] v[+t1.8] = TRiP.HMS00233}attP2* (33361), *y[1] sc[*] v[1]; P{y[+t7.7] v[+t1.8] = TRiP.HMS00617}attP2* (33734), *y[1] v[1]; P{y[+t7.7] v[+t1.8] = TRiP.HMJ02055} attP40* (42491), *y[1] v[1]; P{y[+t7.7] v[+t1.8] = TRiP.JF02336}attP2* (26772), *y[1] v[1]; P{y [+t7.7] v[+t1.8] = TRiP.HMS02020}attP40* (40853), *y[1] sc[*] v[1]; P{y[+t7.7] v[+t1.8] = TRiP. HMS00931}attP2* (33974), *y[1] v[1]; P{y[+t7.7] v[+t1.8] = TRiP.JF02015}attP2* (25993), *y[1] sc[*] v[1]; P{y[+t7.7] v[+t1.8] = TRiP.HMS01054}attP2* (34580), *y[1] sc[*] v[1]; P{y[+t7.7] v[+t1.8] = TRiP.HMS00051}attP2* (34069), *y[1] sc[*] v[1]; P{y[+t7.7] v[+t1.8] = TRiP. HMS00634}attP2/TM3, Sb[1]* (33043), *y[1] sc[*] v[1]; P{y[+t7.7] v[+t1.8] = TRiP.HMC03937} attP40* (55250), *y[1] v[1]; P{y[+t7.7] v[+t1.8] = TRiP.HMC04001}attP40* (55314), *y[1] sc[*] v [1]; P{y[+t7.7] v[+t1.8] = TRiP.HMS00607}attP2* (33725), *y[1] sc[*] v[1]; P{y[+t7.7] v[+t1.8] = TRiP.HMS00076}attP2* (33666), *y[1] v[1]; P{y[+t7.7] v[+t1.8] = TRiP.HMS02334}attP40* (41937), *y[1] v[1]; P{y[+t7.7] v[+t1.8] = TRiP.HMJ21708}attP40* (53697), *y[1] sc[*] v[1]; P{y [+t7.7] v[+t1.8] = TRiP.HMS01387}attP2* (34978), *y[1] v[1]; P{y[+t7.7] v[+t1.8] = TRiP. JF02129}attP2* (26231), *y[1] v[1]; P{y[+t7.7] v[+t1.8] = TRiP.JF02431}attP2* (27085), *y[1] v[1]; P{y[+t7.7] v[+t1.8] = TRiP.JF02231}attP2* (31940), *y[1] v[1]; P{y[+t7.7] v[+t1.8] = TRiP. JF02524}attP2* (29360), *y[1] v[1]; P{y[+t7.7] v[+t1.8] = TRiP.JF02732}attP2* (31960), *y[1] sc[*] v[1]; P{y[+t7.7] v[+t1.8] = TRiP.HMS00628}attP2/TM3, Sb[1]* (32845), *y[1] sc[*] v[1]; P{y [+t7.7] v[+t1.8] = TRiP.HMS01142}attP2* (34665), *y[1] sc[*] v[1]; P{y[+t7.7] v[+t1.8] = TRiP. HMS00586}attP2* (33708), *y[1] sc[*] v[1]; P{y[+t7.7] v[+t1.8] = TRiP.HMS00683}attP2* (32894), *y[1] sc[*] v[1]; P{y[+t7.7] v[+t1.8] = TRiP.HMS00050}attP2* (34520), *y[1] sc[*] v[1]; P{y[+t7.7] v[+t1.8] = TRiP.HMS00684}attP2* (32895), *y[1] sc[*] v[1]; P{y[+t7.7] v[+t1.8] = TRiP. HMS00587}attP2* (33709), *y[1] sc[*] v[1]; P{y[+t7.7] v[+t1.8] = TRiP.HMS00829}attP2* (33891), *y[1] sc[*] v[1]; P{y[+t7.7] v[+t1.8] = TRiP.HMS00301}attP2* (33419), *y[1] sc[*] v[1]; P{y[+t7.7] v[+t1.8] = TRiP.HMS01254}attP2* (34908), *y[1] sc[*] v[1]; P{y[+t7.7] v[+t1.8] = TRiP. HMS00585}attP2* (33707), *y[1] sc[*] v[1]; P{y[+t7.7] v[+t1.8] = TRiP.HMS00302}attP2* (33420).

Genetic interaction tests

Assays for genetic interaction between strains deficient in function for Dom and other chromatin proteins involved RNAi expression mediated via the *Gal4-UAS* system [19]. Crosses were performed at 22°C to adjust *Gal4* expression for detection of genetic interactions. We previously described a recombinant chromosome (*C96-domR*) that contains both a wing margin driver (*C96-Gal4*) and *UAS-dom* RNAi transgenes [14]. This chromosome produces a dominant, but partially-penetrant wing nicking phenotype at 22°C that was validated as a *dom* LOF phenotype. The phenotype is also sensitive to changes in expression of multiple components of the Tip60 complex that contains Dom protein [3], as well as various members of the Notch pathway [14]. Strains containing TRiP (*UAS*-regulated) RNAi transgenes directed against a set of chromatin-associated proteins were each crossed with the *C96-domR* strain. The offspring of these crosses contain *C96-Gal4*- directed expression of both *domR* and tester RNAi transgenes. Control crosses include *C96-domR* mated with w^{1118} flies, for baseline penetrance of the *C96-domR* phenotype, and *C96-Gal4* mated with the tester TRiP strain. The latter cross is used to determine if any wing phenotypes derive from LOF for the TRiP strains alone. In most cases no *C96-Gal4* phenotypes were observed. Therefore, for many assays, genetic interaction could be measured by changes in the penetrance of wing nicking relative to w^{1118} control crosses, either enhancement or suppression. The *C96-domR* x w^{1118} crosses exhibited a range of penetrance from 26%-54%, where wings are scored as positive if they contain one or more anterior margin nicks [14]. Modifiers designated as enhancers or suppressors showed significant differences from control crosses run simultaneously, as determined by a chi-square test. In nearly all cases the significance was high (P< 0.001, see Tables 1 and 2). We express the percent of nicked wings in the experimental vs the control class as a ratio in Tables 1 and 2, where a value greater than 1 (control) is enhancement, and lower than 1 is suppression. Because the control % of nicked wings varied significantly across the experiments, the ratios do not reflect a ranked order of phenotypic severity. We scored all flies emerging from a minimum of eight vials.

Mounting of wings

Wings representative of the average phenotype for each of the strains were mounted onto a slide with Euparol and photographed using a light microscope [12]. The photographs were put in gray scale and sharpened using Adobe Photoshop.

Wing disc antibody staining

Imaginal wing discs were dissected in 1X phosphate buffered saline (PBS), fixed for 20 min in 4% paraformaldehyde, and washed 3 times (1X PBS) prior to being permeablized with 0.3% Triton X-100 in PBS (PBST) for 20 min, and washed once more in 1X PBS [20]. The discs were then incubated overnight at 4°C with 10% normal goat serum (NGS) and primary antibody in 0.1% PBST. Subsequently, the discs were washed 5 times (0.1% PBST) and then incubated overnight at 4°C with NGS and secondary antibody in 0.1% PBST. After the discs were washed 5 more times, they were incubated overnight in n-propyl gallate in glycerol at 4°C, and prepared for confocal microscopy. Images were assembled with Photoshop software (Adobe). Cell death staining used Dcp-1 antibody (1:100, rabbit polyclonal; Cell Signaling) and Alexa 647 secondary antibody (1:100).

Results

Genetic interaction assays between *dom* and other loci encoding chromatin-associated proteins

The *C96-domR* strain constitutively expresses *UAS-dom* RNAi across the dorsal-ventral margin of the wing imaginal disc under *C96-Gal4* control, leading to a dominant and moderately

Table 1. Identification of *dom* modifiers among 30 loci encoding chromatin proteins.

BL #	Name	Effect	Ratio	% E/C	N	*C96-Gal4*
3605	*w1118*	-	1.0	-	>500	-
33981	PCAF	E	3.4	88.3/26	747	-
33962	HP1c	E	2.13	55.3/26	511	-
26234	CC8	E	1.68	91.6/54.4	596	-
31921	JIGR1	E	1.43	75.1/52.4	530	-
42514	CC25	E	1.42	72.7/51.7	478	-
31922	CC20	E	1.38	72.4/52.4	512	-
27085	ERR	E	1.32	57.2/43.3	696	-
33394	RPS9	E	1.26	65.2/52.4	893	-
32888	CC24	E	1.24	50.1/40.4	469	-
33361	CC4	E	1.24	49.9/40.4	503	-
33734	CC7	E	1.2	48.8/40.4	492	-
42491	CC9	E	1.18	55.9/47.4	462	-
26772	CC15	E	1.16	63.3/54.4	695	-
40853	MAF-S	S	0.53	24.9/47.4	473	-
33974	RYBP	S	0.52	21.1/40.4	318	-
25993	CC28	S	0.49	26.9/54.4	360	-
29360	CC32	S	0.48	25.1/52.5	506	-
34580	NUP50	S	0.3	7.7/26	672	-
34069	CAF1	E	3.85	100/26	473	+ (10%)
33043	PCNA	E	3.09	80.3/26	314	+ (1%)
55250	ASF1	E	2.72	70.6/26	260	+ (curling)
55314	TOP1	E	1.42	37/26	653	+ (curling)
33725	RPD3	S	0.27	7.1/26	339	+ (10%/curling)
33666	HEL25E	-	-	-	4	+ (100%)
41937	CC31	-	-	-	44	+ (100%)
53697	SIR2	-	-	-	487	+ (62%)
34978	TRIP1*	-	-	-	26	+ (lethal)
26231	CC34	NE	0.98	50.9/52.2	664	-
31940	CC30	NE	1.03	47.7/46	432	-
31960	DSP1	NE	1.01	26.3/26	623	-

Table 1 shows the Bloomington stock number, gene name and modifier effect on *C96-domR* wing phenotype as Enhancer (E), Suppressor (S), No Effect (NE), or could not be determined (-) for the 30 tested loci. The 23 strains listed as modifiers showed highly significant wing nicking differences from controls (P< 0.001, chi square test). Ratio represents the % nicked wings observed in experimental divided by the control *w1118* (% E/C) in crosses to *C96-domR* run simultaneously. N = # of wings scored. At least 500 *w1118* control cross wings were scored for each assay. *C96-Gal4* column shows results of control crosses to the 30 strains to determine LOF effects. Nine strains showed such effects (+).

*The *TRIP1* cross to *C96-Gal4* was 100% lethal, but a small number of offspring eclosed from the *C96-domR* cross.

penetrant nicked wing phenotype [14]. The *C96-Gal4* transgene contained in the *C96-domR* strain can simultaneously drive other *UAS*-regulated RNAi in transheterozygotes with *UAS-domR*, allowing tests for synergistic effects between the two loci. We investigated loci encoding proteins implicated by others in chromatin binding through various criteria, including the DamID technique [15,16]. This method requires that a tested polypeptide direct bacterial Dam (DNA adenine methyltransferase) close enough to DNA for adenine methylation to occur in a reproducible fashion at specific genomic regions. These investigators analyzed a set of previously defined chromatin proteins, as well as a new set of candidates. They chose candidate loci

Table 2. Identification of *dom* modifiers among 12 other *SWI2/SNF2* loci.

BL #	Name	Effect	Ratio	% E/C	N	*C96-Gal4*
3605	*w¹¹¹⁸*	-	1.0	-	>500	-
32845	*ISWI*	E	2.28	92.3/40	518	-
34665	*CHD1*	E	2.25	82.2/36.5	580	-
33708	*INO80*	E	1.86	67.9/36.5	558	-
32894	*XNP*	E	1.48	54.2/36.5	546	-
34520	*BRM*	E	1.21	44.3/36.5	467	-
32895	*HEL89B*	E	1.20	58.9/49.2	414	-
33709	*MARCAL1*	S	0.89	44/49.6	730	-
33891	*ETL1*	S	0.41	17.4/42.3	448	-
33419	*Mi-2**	E	2.36	100/42.3	5	+ (13%/curling)
34908	*KISMET*	S	0.44	18.6/42.3	290	+ (7.5%)
33420	*CHD3*	NE	0.97	41/42.3	542	-
33707	*OKR*	NE	0.92	38.7/42.3	674	-

Table 2 shows the Bloomington stock number, gene name and modifier effect on *C96-domR* wing phenotype as Enhancer (E), Suppressor (S) or No Effect (NE) for the 12 *SWI2/SNF2* loci. The 10 strains listed as modifiers showed highly significant wing nicking differences from controls (8 strains P< 0.001, chi square test, *MARCAL1*: P< 0.003, Mi-2: P<0.007). Ratio represents the % nicked wings observed in experimental divided by the control *w¹¹¹⁸* (% E/C) in crosses to *C96-domR* run simultaneously. N = # of wings scored. At least 500 *w¹¹¹⁸* control cross wings were scored for each assay. *C96-Gal4* column shows results of control crosses to the 12 strains to determine LOF effects. Two strains showed such effects (+).

*Only 3 flies eclosed from the *Mi-2* x *C96-domR* crosses and 5 wings could be scored, all of which were scalloped severely (Fig 2). The *Mi-2* x *C96-Gal4* control crosses produced 45 offspring, where 12/90 wings contained minor nicks, and 100% were curled.

based on several criteria, including that the proteins contain a domain typically found in chromatin proteins, or alternatively that they interact with a known chromatin protein in a yeast two-hybrid screen. Their DamID study ultimately focused on 70 previously-described chromatin proteins, and 42 newly-characterized proteins that they named chromatin components (CC). We chose 30 strains to analyze, for which *UAS*-regulated TRiP RNAi strains were available from the Bloomington Drosophila Stock Center; 16 strains targeted new candidate CC loci and 14 targeted previously characterized loci encoding chromatin proteins. Three of the CC loci analyzed here are characterized loci not previously known as encoding chromatin components (*JIGR1*, *MAF-S*, *TRIP1*). Females of the *C96-domR* strain were mated to males of each of the 30 TRiP strains, and simultaneously to *w¹¹¹⁸* control males. We also mated *C96-Gal4* driver strain females to males of the TRiP strains to determine if any wing margin effects were produced through LOF for the tester strain alone.

The results for these 30 crosses are summarized in Table 1. This table presents the data for the enhancers followed by the suppressors, first for the loci that did not exhibit a phenotype after the *C96-Gal4* control cross, followed by the loci that did show a phenotype after this cross. We found that 77% (23/30) of the TRiP strains produced either synergistic enhancement or suppression of the *C96-domR* wing nick phenotype. Six strains were suppressors (*MAF-S*, *RYBP*, *CC28*, *CC32*, *NUP50*, *RPD3*), while the remaining 17 were enhancers (*PCAF*, *HP1c*, *CC8*, *JIGR1*, *CC25*, *CC20*, *ERR*, *RPS9*, *CC24*, *CC4*, *CC7*, *CC9*, *CC15*, *CAF1*, *PCNA*, *ASF1*, *TOP1*). The fraction of modifiers detected in the set of new candidate chromatin loci (12/16 = 75%) vs the previously-characterized loci known to encode chromatin proteins (11/14 = 79%) was very similar. Nine of the strains exhibited a phenotype when crossed with *C96-Gal4* alone; phenotypes included wing nicking, wing curling, or near-complete lethality. For five of these nine the phenotypes were minor, allowing scoring of genetic interaction with

dom, as enhancement (*CAF1*, *PCNA*, *ASF1*, *TOP1*), or suppression (*RPD3*). Four of the nine strains (*HEL25E*, *CC31*, *SIR2*, *TRIP1*) could not be scored for interaction with *dom* because of a highly-penetrant wing nick or lethal phenotype. Three strains (*CC34*, *CC30*, *DSP1*) did not display a phenotype via the *C96-Gal4* cross, and also showed no significant modification of the *C96-domR* phenotype.

Representative wings for the 30 crosses, and the *C96-domR/w^{1118}* control are shown in Fig 1. In many cases, enhanced wings show much greater wing nicking penetrance, but otherwise resemble the *C96-domR/w^{1118}* control class in terms of wing blade and margin structure (Fig 1, panels C-N). However, several of the strains that exhibited an effect with *C96-Gal4* alone showed a more severe, synergistic wing blade/margin loss phenotype (Fig 1, panels U, V, W) or a larger structural defect (panel Y) in combination with *C96-domR*. Three strains showed an effect on wing size (Fig 1, panels Z, A2, C2), and in these cases we could only recover a few adult offspring. These three strains could not be assayed for interaction since the *C96-Gal4* control cross phenotype was either 100% penetrant or lethal (Table 1).

Genetic interaction assays between *dom* and other members of the SWI2/SNF2 family

Dom is a member of a family of chromatin modelers and shares the SWI2/SNF2 ATPase domain structure with a group of Drosophila proteins [17]. To investigate potential functional interactions of this larger family with *dom*, we also performed the wing assay with a set of 12 TRiP strains targeting SWI2/SNF2-encoding loci. The results for these 12 crosses are summarized in Table 2. Table 2 presents the data as for Table 1, for enhancers then suppressors, first listing the 10 loci that did not exhibit a phenotype after the *C96-Gal4* control cross, followed by the 2 loci that did show a phenotype after this cross. We observed that 83% (10/12) of the SWI2/SNF2 strains interacted with *C96-domR* as either enhancers (*ISWI*, *CHD1*, *INO80*, *XNP*, *BRM*, *HEL89B*, *Mi-2*) or suppressors (*MARCAL1*, *ETL1*, *KISMET*). Two of the interacting strains showed a phenotype when crossed with *C96-Gal4* alone (*Mi-2*, *KISMET*). The *OKR* and *CHD3* loci did not modify the *C96-domR* phenotype.

Representative wings for the 12 SWI2/SNF2 crosses and controls are shown in Fig 2. We note that the *Mi-2* TRiP strain, which exhibited a weak wing nicking phenotype when driven alone via *C96-Gal4* (13%, Table 2), showed a strong synergistic enhancement of wing nick frequency and wing margin loss when crossed with *C96-domR* (Fig 2M). Moreover, very few flies survived this cross; 3 total flies eclosed from 8 vials, and only 5 wings could be unambiguously scored (Table 2).

Cell death effects underlie a subset of *dom* genetic interactions

The prior associations of *dom* LOF and cell death [1,9] suggested that some of the genetic interactions described above could result from synergism with an apoptosis pathway. Therefore, we examined a subset of modifier crosses by staining wing discs with cleaved Dcp-1 antibody (Fig 3), a marker for apoptosis [21]. Wing discs heterozygous for *C96-Gal4* exhibit occasional random spots of Caspase stain, whereas discs heterozygous for *C96-domR* show weak staining aligned with a portion of the dorsal-ventral wing margin (Fig 3A and 3B). When *C96-Gal4* is used to drive *CAF1* RNAi alone a weak Caspase stain is evident across the margin (Fig 3C), whereas the *C96-domR + CAF1* genotype leads to strong synergistic Caspase staining across the margin (Fig 3D). The extensive cell death evident across the margin reflects the striking loss of anterior and posterior wing margins observed in adult wings (Fig 1U). Similar analysis with the *ASF1* enhancer showed background levels of Caspase staining in the *C96-Gal4 + ASF1* discs and moderately strong staining in *C96-domR + ASF1* discs (Fig 3E and 3F); again
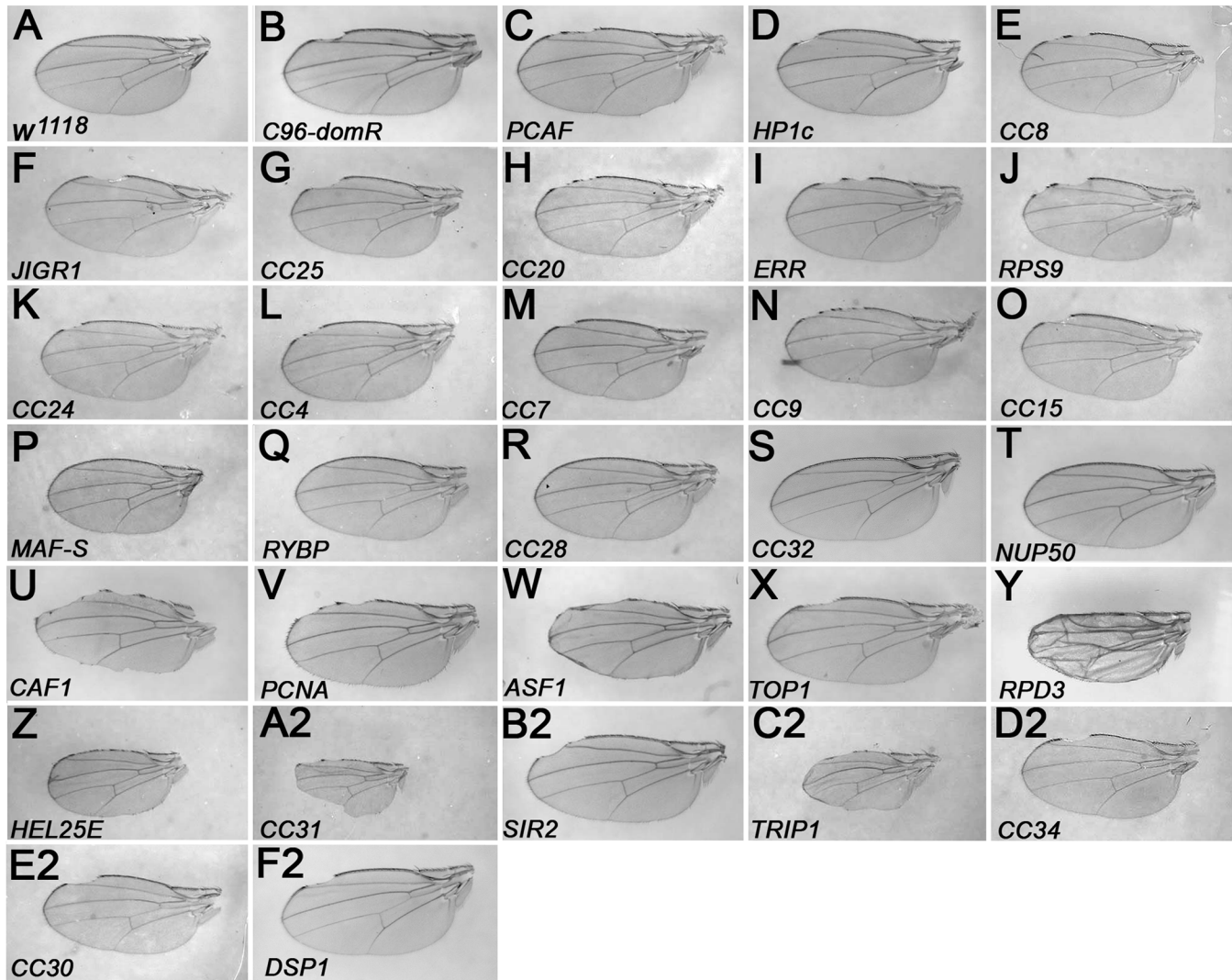
Fig 1. Genetic interactions of 30 chromatin protein encoding loci with *domino*. Wing mounts were prepared from the following Bloomington (BL) strains after crosses to *C96-domR*. Wings shown in panels C-F2 derived from crosses to TRiP strains. A. Wild Type wing BL3605 w^{1118}, B. Control wing *C96-domR/ w^{1118}*, C. BL33981 *PCAF*, D. BL33962 *HP1c*, E. BL26234 *CC8*, F. BL31921 *JIGR1*, G. BL42514 *CC25*, H. BL31922 *CC20* I. BL27085 *ERR*, J. BL33394 *RPS9*, K. BL32888 *CC24*, L. BL33361 *CC4*, M. BL33734 *CC7*, N. BL42491 *CC9*, O. BL26772 *CC15*, P. BL40853 *MAF-S*, Q. BL33974 *RYBP*, R. BL25993 *CC28*, S. BL29360 *CC32*, T. BL34580 *NUP50*, U. BL34069 *CAF1*, V. BL33043 *PCNA*, W. BL55250 *ASF1*, X. BL55314 *TOP1*, Y. BL33725 *RPD3*, Z. BL33666 *HEL25E*, A2. BL41937 *CC31*, B2. BL53697 *SIR2*, C2. BL34978 *TRIP1*, D2. BL26231 *CC34*, E2. BL31940 *CC30*, F2. BL31960 *DSP1*

doi:10.1371/journal.pone.0142635.g001

consistent with synergism evident in the adult wing phenotype ([Fig 1W](#)). *CC31* exhibited a small wing and 100% penetrant wing nicking phenotype when crossed with *C96-Gal4* alone (data not shown), or in combination with *C96-domR* ([Fig 1](#)A2); this precluded our ability to score for a genetic interaction in adult wings. However, we detected high levels of Caspase across the wing margin in *C96-Gal4 + CC31* discs, and significantly higher levels of stain in *C96-domR + CC31* discs ([Fig 3G and 3H](#)), suggesting a synergistic effect. *RPD3* RNAi produced curled wings and exhibited nicks in 10% of the wings when driven by *C96-Gal4*; paradoxically, *RPD3* RNAi strongly suppressed the *C96-domR* wing nicking phenotype ([Table 1](#)). We compared Caspase stain levels from these crosses and observed strong staining in *C96-Gal4 + RPD3* discs, but suppressed levels in *C96-domR + RPD3* discs ([Fig 3I and 3J](#)). We also note that adult wings derived from the latter cross exhibit an additional phenotype, as the dorsal
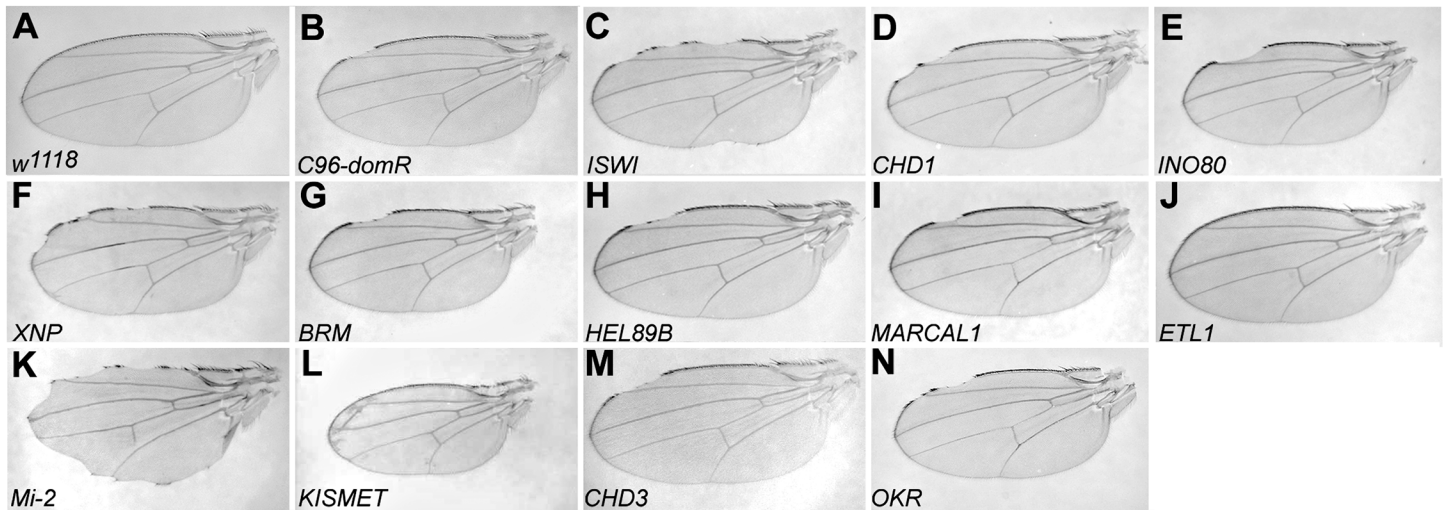
Fig 2. Genetic interactions of 12 SWI2/SNF2 protein encoding loci with *domino*. Wing mounts were prepared from the following Bloomington (BL) strains after crosses to *C96-domR*. Wings shown in panels C-N derived from crosses to TRiP strains. A. Wild Type wing BL3605 *w¹¹¹⁸*, B. Control wing *C96-domR/w¹¹¹⁸*, C. BL32845 *ISWI*, D. BL34665 *CHD1*, E. BL33708 *INO80*, F. BL32894 *XNP*, G. BL34520 *BRM*, H. BL32895 *HEL89B*, I. BL33709 *MARCAL1*, J. BL33891 *ETL1*, K.BL33419 *Mi-2*, L. BL34908 *KISMET*, M. BL33420 *CHD3*, N. BL33707 *OKR*.

and ventral wing surfaces are not adhered properly, leading to a disorganized structure (Fig 1Y). Therefore, the combined LOF for both *dom* and *RPD3* at the margin lead to more widespread effects. Finally, we compared Caspase stain levels in discs from *C96-Gal4 + PCNA* and *C96-domR + PCNA* discs (Fig 3K and 3L). Despite showing strong enhancement of *C96-domR* wing nicking frequency (Table 1), *PCNA* RNAi does not lead to elevated Caspase stain levels in either genotype. Therefore, a subset of the genetic interactions we observe with *dom* can be measured in terms of cell death changes.

Discussion

The initial molecular and genetic characterizations of *dom* linked it to chromatin remodeling and repression of homeotic loci, and showed a strong effect on cell viability and proliferation [1,2]. Subsequent studies demonstrated that *dom* plays a broad role during development and functions in both positive and negative regulation [12,4,13,10,14], at least in part through its role in the Tip60 complex [3]. Loss of *dom* function has also been shown to alter the expression of multiple genes [11], one of which was assayed (see below). The results reported here extend these studies, and reveal that *dom* function intersects with the activity of many other chromatin-associated proteins. It is noteworthy that under 22°C conditions, the majority of loci tested did not exhibit an RNAi-mediated LOF phenotype when tested in *Gal4* control crosses, but did synergize with *dom* (26/31 strains = 84%; Tables 1 and 2). Therefore, expression of *dom* RNAi across the dorsal-ventral margin apparently sensitizes the wing to loss of other regulatory inputs. These inputs likely impinge on major cell pathways; as described below, numerous modifier loci have been associated with cell proliferation/cell cycle, cell death and Notch signaling. This is not unexpected given that many of these chromatin component loci are well-described global regulators that localize to a large number of genomic sites [17,15,16].

For example, among the previously-characterized class of chromatin factors [15,16], *CAF1* was the strongest enhancer detected. CAF1 (chromatin assembly factor 1) is a component (NURF55) of the nucleosome remodeling factor complex that regulates cell death and proliferation and Notch signaling [22,23,24]. *CAF1* LOF has been shown to elevate apoptosis in eye
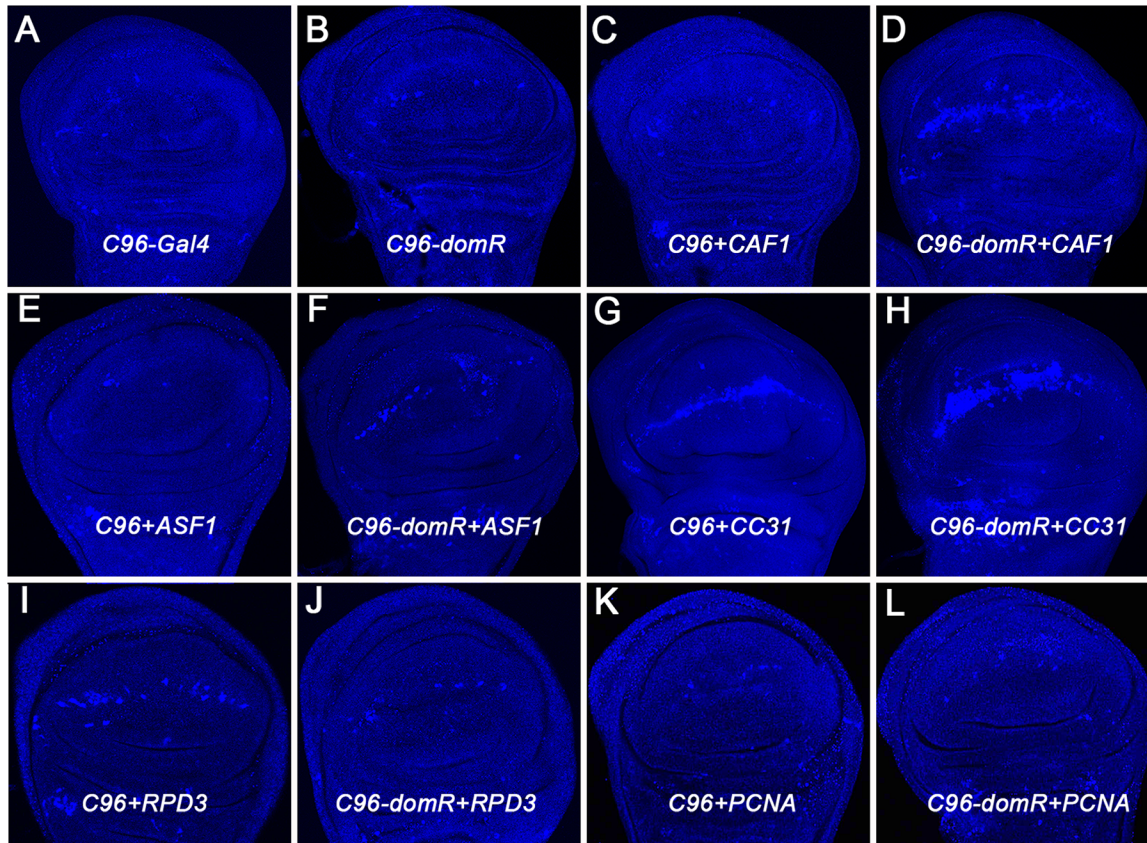
Fig 3. Cell death effects. Imaginal wing discs from following genotypes were stained with Dcp-1 antisera to measure caspase activity. A. Control *C96-Gal4/*
+ heterozygote shows occasional random stain, B. Control *C96-domR/+* heterozygote shows minor staining across dorsal-ventral wing margin, C. *C96-Gal4*
+Caf1, D. *C96-domR+Caf1*, E. *C96-Gal4+ASF1*, F. *C96-domR+ASF1*, G. *C96-Gal4+CC31*, H. *C96-domR+CC31*, I. *C96-Gal4+RPD3*, J. *C96-domR+RPD3*,
K. *C96-Gal4+PCNA*, L. *C96-domR+PCNA*.

doi:10.1371/journal.pone.0142635.g003

discs [23], and we observed elevated levels of cell death across the margin of *C96-Gal4+CAF1*
discs, and strong synergism in cell death levels when *CAF1* and *dom* LOF were combined (Fig 3). *PCAF* (*dGCN5*, P300/CBP-associated factor), another strong enhancer, is a histone acetyl-transferase (HAT) that also functions with Notch, and affects cell proliferation in the wing [25]. The *ERR* (estrogen-related receptor) locus enhanced strongly, and it has also been implicated in proliferation [26]; further, we showed previously that another nuclear receptor locus (*EcR*) interacts with *dom* similarly [14]. The *PCNA* (proliferating cell nuclear antigen) locus likely enhances primarily due to effects on efficiency of DNA replication/cell division [27], and we observe no elevation of apoptosis in wing discs deficient for *PCNA* and *dom* (Fig 3). Enhancement via loss of HP1c function may derive from an effect on RNA polymerase elongation [28], thereby generally reducing gene expression levels. HP1c appears to be an atypical, positive transcriptional effector within the HP1 protein group, which typically mark inactive heterochromatic regions of the genome [15]. The *ASF1* (*Anti Silencing Factor*/histone chaperone) and *TOP1* (topoisomerase) enhancers each have effects on transcription and replication [29,30], and ASF1 has also been associated with Notch signaling [31], as well as a *tousled-like kinase* pathway preventing cell death [32]. The latter is consistent with the increased cell death evident in *dom+ASF1* wing discs (Fig 3).

Among the previously-described chromatin factors we also detected three suppressors.
RPD3 (*HDAC1*) encodes a histone deacetylase that has been directly connected to gene

repression, and LOF for *RPD3* was associated with elevated expression of Notch pathway targets [31]. Activation of Notch has been demonstrated to suppress apoptosis [33]. These effects could explain the suppressive effect of *RPD3* LOF observed here Table 1, Figs 1 and 3), since an activated form of Notch was shown to rescue the *dom* LOF wing phenotype [14]. *NUP50* encodes a nucleoporin and it is possible that the interaction with *dom* reflects a more general effect on nuclear transport or association of pores with chromatin [16]. The *RYBP* locus (ring and YY1 binding protein) encodes a Zn-finger protein that elicits a wide range of defects during embryonic and imaginal development, including effects on cell division [34].

We also tested a group of 16 loci that were not previously associated with chromatin, but found by DamID to bind specific chromosomal regions [16]. Our assay included 13 of these "chromatin component" (CC) loci and three additional loci that were studied in different contexts, but not as chromatin components (*JIGR1, MAF-S, TRIP1*) prior to this analysis [16]. As several of these loci are relatively uncharacterized beyond their predicted sequence or physical binding partners, genetic descriptions are limited.

We found that 4 moderate *dom* enhancers, that showed no effect when assayed for LOF alone in control crosses (*CC8, JIGR1, CC25,* and *CC20*), all contain a MADF (Myb/SANT-like Domain in Adf-1) DNA-binding domain. An additional locus (*CC34*) also encodes this domain, but did not show an interaction. The MADF domain is similar to the SANT domain (a domain found in Dom, as well as ISWI and BRM), and was first identified in the transcriptional activator, Adh transcription factor 1 (Adf-1). Proteins with the MADF domain have been found to act as both activators and repressors [35]. It may be relevant that 4 of the 5 proteins in our study that contain a MADF domain behaved similarly in the assay for *dom* modification (Table 1). For example, LOF for *CC20* affects wing hinge structure [35], as is the case for *dom* LOF, which produces a held out wing phenotype in adults carrying very weak *dom* alleles [2]. Likewise, *JIGR1* was scored among the positives in a screen for genes that were upregulated by RAS expression in hyper-proliferating hemocytes [36]. Although *dom* was not scored in this screen, the role of *dom* in hemocytes is well described [1], thus the function of these loci could intersect in hemocytes. Additionally, the *dom* enhancer *CC9* was also scored as a positive in this screen [36], however *CC9*, which is relatively uncharacterized, does not encode a MADF-containing protein.

A few additional modifiers exhibit other features that indicate an overlap in function with *dom*. The *CC15* locus encodes a Zn-finger protein, and it was detected as a significant enhancer of *dom*. Prior RNAi knockdown studies of *CC15* demonstrated effects on cell cycle progression, increased cell death, and a held out wing phenotype [37]. The CC32 locus was scored as a strong *dom* suppressor. It also encodes a Zn-finger protein that was found in a screen for novel genes involved in hematopoiesis [38]. *MAF-S*, scored as a moderate suppressor of *dom*, has been shown to modulate Myc-induced growth [39]. The remaining four modifiers (*CC4, CC7, CC24, CC28*) encode proteins with known domains that associate with chromatin, and they have been mapped by DamID to regions of active loci (*CC7, CC24, CC28*) or inactive loci (CC4) [16]; however there is not sufficient information available on these loci to infer a further relationship to *dom*. We do note however a report [11] that the expression of the CC24 transcript is diminished in *dom* mutant larvae, which is consistent with the phenotypic enhancement effect we observe (Table 1). Three of the tested loci did not show significant modification of the *dom* phenotype (*CC34, CC30* and *DSP1*), and four additional loci (*HEL25E, CC31, SIR2, TRIP1*) produced highly-penetrant LOF phenotypes in a wild type *dom* background (Table 1, *C96-Gal4* column) that precluded scoring a *dom* LOF interaction in adult wings. However, we did examine *CC31* further for an effect on cell death. *CC31* codes for a zinc finger protein, Motif 1 binding protein (M1BP) that is required for cell viability and proliferation [40]. In both the *C96-domR* and *C96-Gal4* crosses *CC31* LOF resulted in 100% wing nicking, and a

substantially smaller wing ([Table 1](), [Fig 1]()). We observed that *C96-Gal4+CC31* wing discs exhibited high levels of apoptosis across the margin, and that even higher levels were apparent when *CC31* was combined with *dom* LOF ([Fig 3]()), indicating again a synergistic interaction between these loci.

Since Dom is a member of the SWI2/SNF2 protein family we also investigated genetic interactions with a set of TRiP RNAi strains that target 12 other family members. The SWI2/SNF2 chromatin remodelers act in numerous contexts, including transcription, replication, DNA repair, recombination and chromosome segregation [41]. We reasoned that Dom could function in related pathways and tissues, or act redundantly with other SWI2/SNF2 proteins; either of these possibilities may be detected through genetic interaction studies. We found that 83% (10/12) of the tested loci elicited a significant modification to the *dom* wing phenotype, whereas only two of these 10 exhibited an RNAi-mediated phenotype in control crosses ([Table 2]()).

The early phenotypic descriptions of *dom* alleles implicated the locus in immunity/hematopoiesis and homeotic gene regulation [1,2]. Four of the modifiers: *ISWI*, *CHD1*, *HEL89B* and *ETL1* affect immunity or hemocyte number [42,43,44], whereas five have been described as homeotic regulators: *ISWI*, *INO80*, *BRM*, *Mi-2* and *KISMET* [45,46,2,47,48]. We reported previously that *dom* has a role in Notch signaling [12,14], and *ISWI*, *CHD1*, *BRM* and *KISMET* have also been shown to interact with *Notch* or lead to nicked wings when mutated [49,50,51]. Finally, the role of Dom within the Tip60 complex at double stranded DNA breaks revealed a role in DNA repair through acetylation and exchange of phosphorylated histone H2Ax(v) [3]. *INO80* and *MARCAL1* have also been implicated in repair [41,52,53].

In conclusion, it is perhaps not surprising that a substantial fraction of loci encoding chromatin-associated proteins was found to intersect with *dom* function, as this may reflect the broad realms of function and collaboration among these regulatory genes. As described earlier, Dom has been associated with many fundamental cell processes, including cell proliferation, cell viability/death, autophagy, Notch signaling and both positive and negative gene regulation through its participation in the Tip60 complex. Moreover, LOF for *dom* has been associated with widespread changes in gene activity [11]. The complexity of genetic interactions between *dom* and other loci that intersect with these pathways is illustrated by *Notch*. In some contexts Notch signaling can induce cell proliferation [54] and block cell death [33]. As Dom appears to be a positive effector of Notch signaling [12,4,13,14], these observations are consistent with the original phenotypic descriptions of *dom* alleles [1,2]. However, Dom has also been characterized as a repressor of E2F-responsive loci, and therefore a negative factor in cell proliferation control [10]. Loss of function for *dom* also synergizes with genotypes depressed in autophagy pathway activity [14], and the well-described antagonistic interactions between the autophagy and cell death pathways [55] may add further complexity to these phenotypes. Consequently, interpreting genetic interactions among loci that network with Dom must be done cautiously, since the interactions likely reflect substantial pleiotropic effects.

Acknowledgments

Author Contributions

Conceived and designed the experiments: BY. Performed the experiments: KE CF. Analyzed the data: KE CF BY. Wrote the paper: BY.

References

1. Braun A, Lemaitre B, Lanot R, Zachary D, Meister M. Drosophila immunity: analysis of larval hemocytes by P-element-mediated enhancer trap. Genetics. 1997 Oct; 147(2):623–34. PMID: 9335599

2. Ruhf ML, Braun A, Papoulas O, Tamkun JW, Randsholt N, Meister M. The domino gene of Drosophila encodes novel members of the SWI2/SNF2 family of DNA-dependent ATPases, which contribute to the silencing of homeotic genes. Development. 2001 Apr; 128(8):1429–41. PMID: 11262242

3. Kusch T, Florens L, Macdonlad WH, Swanson SK, Glaser RL, Yates JR 3rd, et al. Acetylation by Tip60 is required for selective histone variant exchange at DNA lesions. Science. 2004 Dec 17; 306 (5704):2084–7. PMID: 15528408

4. Eissenberg JC, Wong M, Chrivia JC. Human SRCAP and Drosophila melanogaster DOM are homologs that function in the notch signaling pathway. Mol Cell Biol. 2005 Aug; 25(15):6559–69. PMID: 16024792

5. Sterner DE, Berger SL. Acetylation of histones and transcription-related factors. Microbiol Mol Biol Rev. 2000 Jun; 64(2):435–59. PMID: 10839822

6. Bararia D, Trivedi AK, Zada AA, Greif PA, Mulaw MA, Christopeit M, et al. Proteomic identification of the MYST domain histone acetyltransferase TIP60 (HTATIP) as a co-activator of the myeloid transcription factor C/EBPalpha. Leukemia. 2008 Apr; 22(4):800–7. doi: 10.1038/sj.leu.2405101 PMID: 18239623

7. Qi D, Jin H, Lilja T, Mannervik M. Drosophila Reptin and other Tip60 complex components promote generation of silent chromatin. Genetics. 2006 Sep; 174(1):241–51. PMID: 16816423

8. Xi R, Xie T. Stem cell self-renewal controlled by chromatin remodeling factors. Science. 2005 Dec 2; 310(5753):1487–9. PMID: 16322456

9. Yan D, Neumuller RA, Buckner M, Ayers K, Li H, Hu Y, et al. A regulatory network of Drosophila germline stem cell self-renewal. Dev Cell. 2014 Feb 24; 28(4):459–73. doi: 10.1016/j.devcel.2014.01.020 PMID: 24576427

10. Lu J, Rhuf ML, Perrimon N, Leder P. A genome-wide RNA interference screen identifies putative chromatin regulators essential for E2F repression. Proc Natl Acad Sci USA. 2007 May 29; 104(22):9381–6. PMID: 17517653

11. Walker J, Kwon SY, Badenhorst P, East P, McNeill H, Svejstrup JQ. Role of elongator subunit Elp3 in Drosophila melanogaster larval development and immunity. Genetics. 2011 Apr; 187(4):1067–75. doi: 10.1534/genetics.110.123893 PMID: 21288872

12. Hall LE, Alexander SJ, Chang M, Woodling NS, Yedvobnick B. An EP overexpression screen for genetic modifiers of Notch pathway function in Drosophila melanogaster. Genet Res. 2004 Apr; 83 (2):71–82. PMID: 15219152

13. Gause M, Eissenberg JC, Macrae AF, Dorsett M, Misulovin Z, Dorsett D. Nipped-A, the Tra1/TRRAP subunit of the Drosophila SAGA and Tip60 complexes, has multiple roles in Notch signaling during wing development. Mol Cell Biol. 2006 Mar; 26(6):2347–59. PMID: 16508010

14. Kwon MH, Callaway H, Zhong J, Yedvobnick B. A targeted genetic modifier screen links the SWI2/SNF2 protein domino to growth and autophagy genes in Drosophila melanogaster. G3 (Bethesda). 2013 May 20; 3(5):815–25.

15. Filion GJ, van Bemmel JG, Braunschweig U, Talhout W, Kind J, Ward LD, et al. Systematic protein location mapping reveals five principal chromatin types in Drosophila cells. Cell. 2010 Oct 15; 143 (2):212–24. doi: 10.1016/j.cell.2010.09.009 PMID: 20888037

16. van Bemmel JG, Filion GJ, Rosado A, Talhout W, de Haas M, van Welsem T, et al. A network model of the molecular organization of chromatin in Drosophila. Mol Cell. 2013 Feb 21; 49(4):759–71. doi: 10.1016/j.molcel.2013.01.040 PMID: 23438860

17. Schneiderman JI, Sakai A, Goldstein S, Ahmad K. The XNP remodeler targets dynamic chromatin in Drosophila. Proc Natl Acad Sci USA. 2009 Aug 25; 106(34):14472–7. doi: 10.1073/pnas.0905816106 PMID: 19706533

18. Helms W, Lee H, Ammerman M, Parks AL, Muskavitch MA, Yedvobnick B. Engineered truncations in the Drosophila mastermind protein disrupt Notch pathway function. Dev Biol. 1999 Nov 15: 215 (2):358–74. PMID: 10545243

19. Brand AH, Perrimon N. Targeted gene expression as a means of altering cell fates and generating dominant phenotypes. Development. 1993 Jun; 118(2):401–15. PMID: 8223268

20. Moberg KH, Schelble S, Burdick SK, Hariharan IK. Mutations in erupted, the Drosophila ortholog of mammalian tumor susceptibility gene 101, elicit non-cell-autonomous overgrowth. Dev Cell. 2005 Nov: 9:699–710. PMID: 16256744

21. Fan Y, Bergmann A. The cleaved-Caspase-3 antibody is a marker of Caspase-9-like DRONC activity in Drosophila. Cell Death Differ. 2010 Mar; 17(3):534–9. doi: 10.1038/cdd.2009.185 PMID: 19960024

22. Collins H, Moon NS. The components of Drosophila histone chaperone dCAF-1 are required for the cell death phenotype associated with rbf1 mutation. G3 (Bethseda). 2013 Oct 3; 3(10):1639–47.

23. Anderson AE, Karandikar UC, Pepple KL, Chen Z, Bergmann A, Mardon G. The enhancer of trithorax and polycomb gene Caf1/p55 is essential for cell survival and patterning in Drosophila development. Development. 2011 May; 138(10):1957–66. doi: 10.1242/dev.058461 PMID: 21490066

24. Yu Z, Wu H, Chen H, Wang R, Liang X, Liu J, et al. CAF-1 promotes Notch signaling through epidemic control of target gene expression during Drosophila development. Development. 2013 Sep 1; 140 (17):3635–44. doi: 10.1242/dev.094599 PMID: 23942516

25. Carre C, Szymczak D, Pidoux J, Antoniewski C. The histone H3 acetylase dGcn5 is a key player in Drosophila melanogaster metamorphosis. Mol Cell Biol. 2005 Sep; 25(18):8228–38. PMID: 16135811

26. Tennessen JM, Baker KD, Lam G, Evans J, Thummel CS. The Drosophila estrogen-related receptor directs a metabolic switch that supports developmental growth. Cell Metab. 2011 Feb 2; 13(2):139–48. doi: 10.1016/j.cmet.2011.01.005 PMID: 21284981

27. Kolesnikova TD, Posukh OV, Andreyeva EN, Bebyakina DS, Ivankin AV, Zhimulev IF. Drosophila SUUR protein associates with PCNA and binds chromatin in a cell cycle-dependent manner. Chromosoma. 2013 Mar; 122(1–2):55–66. doi: 10.1007/s00412-012-0390-9 PMID: 23149855

28. Kwon SH, Workman JL. HP1c casts light on dark matter. Cell Cycle. 2011 Feb 15; 10(4):625–30. PMID: 21301224

29. Zhang CX, Chen AD, Gettel NJ, Hsieh TS. Essential functions of DNA topoisomerase I in Drosophila melanogaster. Dev Biol. 2000 Jun 1; 222(1):27–40. PMID: 10885744

30. Schulz LL, Tyler JK. The histone chaperone ASF1 localizes to active DNA replication forks to mediate efficient DNA replication. FASEB J. 2006 Mar; 20(3):488–90. PMID: 16396992

31. Moshkin YM, Kan TW, Goodfellow H, Bezstarosti K, Maeda RK, Pilyugin M, et al. Histone chaperones ASF1 and NAP1 differentially modulate removal of active histone marks by LID-RPD3 complexes during NOTCH silencing. Mol Cell. 2009 Sep 24; 35(6):782–93. doi: 10.1016/j.molcel.2009.07.020 PMID: 19782028

32. Carrera P, Moshkin YM, Gronke S, Sillje HH, Nigg EA, Jackle H, et al. Tousled-like kinase functions with the chromatin assembly pathway regulating nuclear divisions. Genes Dev. 2003 Oct 15; 17 (20):2578–90. PMID: 14561777

33. Ye Y, Fortini ME. Apoptotic activities of wild-type and Alzheimer's disease-related mutant presenilins in Drosophila melanogaster. J Cell Biol. 1999 Sep 20; 146(6):1351–64. PMID: 10491396

34. Gonzalez I, Aparicio R, Busturia A. Functional characterization of the dRYBP gene in Drosophila. Genetics. 2008 Jul; 179(3):1373–88. doi: 10.1534/genetics.107.082966 PMID: 18562658

35. Shukla V, Habib F, Kulkarni A, Ratnaparkhi GS. Gene duplication, lineage-specific expansion, and subfunctionalization in the MADF-BESS family patterns the Drosophila wing hinge. Genetics. 2014 Feb; 196(2):481–96. doi: 10.1534/genetics.113.160531 PMID: 24336749

36. Asha H, Nagy I, Kovacs G, Stetson D, Ando I, Dearolf CR. Analysis of Ras-induced overproliferation in Drosophila hemocytes. Genetics. 2003 Jan: 163(1):203–15. PMID: 12586708

37. Zaytseva O, Tenis N, Mitchell N, Kanno S, Yasui A, Heierhorst J, et al. The novel zinc finger protein dASCIZ regulates mitosis in Drosophila via an essential role in dynein light-chain expression. Genetics. 2014 Feb; 196(2):443–53. doi: 10.1534/genetics.113.159541 PMID: 24336747

38. Mondal BC, Shim J, Evans CJ, Banerjee U. Pvr expression regulators in equilibrium signal control and maintenance of Drosophila blood progenitors. Elife. 2014 Sep 8; 3:e03626. doi: 10.7554/eLife.03626 PMID: 25201876

39. Nagy P, Varga A, Pircs K, Hegedus K, Juhasz G. Myc-driven overgrowth requires unfolded protein response-mediated induction of autophagy and antioxidant responses in Drosophila melanogaster. PLoS Genet. 2013; 9(8):e1003664. doi: 10.1371/journal.pgen.1003664 Epub 2013 Aug 8. PMID: 23950728

40. Li J, Gilmour DS. Distinct mechanisms of transcriptional pausing orchestrated by GAGA factor and M1BP, a novel transcription factor. EMBO J. 2013 Jul 3; 32(13):1829–41. doi: 10.1038/emboj.2013.111 PMID: 23708796

41. Clapier CR, Cairns BR. The biology of chromatin remodeling complexes. Annu Rev Biochem. 2009; 78:273–304. doi: 10.1146/annurev.biochem.77.062706.153223 PMID: 19355820

42. Yagi Y, Ip YT. Helicase89B is a Mot1p/BTAF1 homologue that mediates an antimicrobial response in Drosophila. EMBO Rep. 2005 Nov; 6(11):1088–94. PMID: 16200050

43. Cronin SJ, Nehme NT, Limmer S, Liegeois S, Pospisilik JA, Schramek D. et al. Genome-wide RNAi screen identifies genes involved in intestinal pathogenic bacterial infection. Science. 2009 Jul 17; 325 (5938):340–3. doi: 10.1126/science.1173164 PMID: 19520911

44. Sebald J, Morettini S, Podhraski V, Lass-Florl C, Lusser A. CHD1 contributes to intestinal resistance against infection by P. aeruginosa in Drosophila melanogaster. PLoS One. 2012; 7(8):e43144. doi: 10.1371/journal.pone.0043144 PMID: 22912810

45. Kennison JA, Tamkun JW. Dosage-dependent modifiers of polycomb and antennapedia mutations in Drosophila. Proc Natl Acad Sci USA. 1988 Nov; 85(21):8136–40. PMID: 3141923

46. Kehle J, Beuchle D, Treuheit S, Christen B, Kennison JA, Bienz M, et al. dMi-2, a hunchback-interacting protein that functions in polycomb repression. Science. 1998 Dec 4; 282(5395):1897–900. PMID: 9836641

47. Badenhorst P, Voas M, Rebay I, Wu C. Biological functions of the ISWI chromatin remodeling complex NURF. Genes Dev. 2002 Dec 15; 16(24):3186–98. PMID: 12502740

48. Bhatia S, Pawar H, Dasari V, Mishra RK, Chandrashekaran S, Brahmachari V. Chromatin remodeling protein INO80 has a role in regulation of homeotic gene expression in Drosophila. Genes Cells. 2010 Jun; 15(7):725–35. doi: 10.1111/j.1365-2443.2010.01416.x PMID: 20545766

49. Verheyen EM, Purcell KJ, Fortini ME, Artavanis-Tsakonas S. Analysis of dominant enhancers and suppressors of activated Notch in Drosophila. Genetics. 1996 Nov: 144(3):1127–41. PMID: 8913755

50. Armstrong JA, Sperling AS, Deuring R, Manning L, Moseley SL, Papoulas O, et al. Genetic screens for enhancers of brahma reveal functional interactions between the BRM chromatin-remodleing complex and the delta-notch signal transduction pathway in Drosophila. Genetics. 2005 Aug; 170(4):1761–74. PMID: 15944353

51. McDaniel IE, Lee JM, Berger MS, Hanagami CK, Armstrong JA. Investigations of CHD1 function in transcription and development of Drosophila melanogaster. Genetics. 2008 Jan; 178(1):583–7. doi: 10.1534/genetics.107.079038 PMID: 18202396

52. Kassavetis GA, Kadonaga JT. The annealing helicase and branch migration activities of Drosophila HARP. PLoS One. 2014 May 27; 9(5):e98173. doi: 10.1371/journal.pone.0098173 PMID: 24866343

53. Dekanty A, Barrio L, Milan M. Contributions of DNA repair, cell cycle checkpoints and cell death to suppressing the DNA damage-induced tumorigenic behavior of Drosophila epithelial cells. Oncogene. 2015 Feb 19; 34(8):978–85. doi: 10.1038/onc.2014.42 PMID: 24632609

54. Giraldez AJ, Cohen SM. Wingless and Notch signaling provide cell survival cues and control cell proliferation during wing development. Development. 2003 Dec; 130(26):6533–43. PMID: 14660542

55. Gordy C, He YW. The crosstalk between autophagy and apoptosis: where does this lead? Protein Cell. 2012 Jan; 3(1):17–27. doi: 10.1007/s13238-011-1127-x PMID: 22314807